IRSTI 53.37.35; 53.39.03 https://doi.org/10.26577/RCPh97220264

Ye. Kenzhin[1], T. Kulsartov[1], I. Kenzhina[1*], Zh. Zaurbekova[1],
K. Samarkhanov[2], S. Udartsev[1,3], A. Yelishenkov[1], G. Kantay[4]
[1]Satbayev University, Almaty, Kazakhstan
[2]Institute of Atomic Energy Branch of the National Nuclear Center of the Republic of Kazakhstan, Kurchatov, Kazakhstan
[3]JSC "Ulba Metallurgical Plant", Ust'-Kamenogorsk, Kazakhstan
[4]Institute of Physics of the Slovak Academy of Sciences, Bratislava, Slovakia
*e-mail: kenzhina@physics.kz

# THERMAL DESORPTION BEHAVIOR OF HOLMIUM AND ERBIUM HYDRIDE POWDERS UNDER VACUUM HEATING

The study investigates the thermal desorption behavior of holmium and erbium hydride powders during heating under vacuum to determine well-founded temperature–time parameters for the subsequent synthesis of lanthanide beryllides. The relevance of this study is determined by the need to account for gas evolution from hydride-containing powder mixtures during vacuum thermal treatment, since hydrogen desorption can significantly affect powder densification, vacuum stability, and phase formation conditions.

Before the thermal desorption (TDS) experiments, the initial powders of beryllium, holmium hydride, and erbium hydride were characterized, including analysis of particle size distribution, particle morphology, and phase composition. TDS studies were carried out under vacuum conditions with linear heating from room temperature to 1173 K at a rate of 10 K/min. It is shown that heating of holmium and erbium hydride powders results in a multistage character with a dominant high-temperature peak.

The obtained results make it possible to determine the temperature ranges of the most intense gas evolution and can be used to justify vacuum heating regimes during the preparation and implementation of experiments on the synthesis of lanthanide beryllides from powder mixtures based on beryllium and rare-earth metals.

**Keywords:** rare-earth metals, metal hydrides, thermal desorption spectroscopy (TDS), powder materials, vacuum heating, hydrogen desorption.

Е. Кенжин[1], Т. Кульсартов[1], И. Кенжина[1*], Ж. Заурбекова[1],
Қ. Самарханов[2], С. Ударцев[1,3], А. Елишенков[1], Г. Қантай[4]
[1]Қ.И. Сәтбаев атындағы ҚазҰТЗУ КеАҚ, Алматы, Қазақстан
[2]Қазақстан Республикасы Ұлттық ядролық орталығының Атом энергиясы институты филиалы, Курчатов, Қазақстан
[3]"Үлбі металлургиялық зауыты" АҚ, Өскемен, Қазақстан
[4]Словакия ғылым академиясының Физика институты, Братислава, Словакия
*e-mail: kenzhina@physics.kz

# Вакуум жағдайында қыздыру кезінде гольмий мен эрбий гидриді ұнтақтарының термодесорбциялық сипаттамалары

Бұл жұмыста вакуумда қыздыру кезінде гольмий және эрбий гидридтері ұнтақтарының термодесорбциялық (ТДС) сипаттамалары зерттеліп, лантаноид бериллидтерін кейінгі синтездеу үшін негізделген температура-уақыт параметрлерін таңдау мақсаты қойылды. Зерттеудің өзектілігі вакуумдық-термиялық қыздыру барысында гидрид құрамды ұнтақ қоспаларынан газ бөлінуін ескеру қажеттілігімен анықталады, өйткені сутегінің десорбциясы қоспаның тығыздалуына, вакуум режимінің тұрақтылығына және фазалардың түзілу шарттарына елеулі әсер етуі мүмкін.

 

ТДС зерттеулерді жүргізер алдында бастапқы бериллий, гольмий гидриді және эрбий гидриді ұнтақтарына сипаттама берілді, оған гранулометриялық құрамын, бөлшек морфологиясын және фазалық күйін талдау кірді. ТДС зерттеулер вакуум жағдайында бөлме температурасынан 1173 К-ге дейін 10 К/мин жылдамдықпен қыздыру арқылы жүргізілді. Гольмий және эрбий гидридтері ұнтақтарын қыздыру кезінде сутегінің бөлінуі жоғары температура аймағында басым максимумымен сипатталатын көпсатылы сипат.

Алынған нәтижелер қарқынды газ бөлінуі байқалатын температуралық аралықтарды анықтауға мүмкіндік береді және бериллий мен сирек жер металдары негізіндегі ұнтақ қоспаларынан лантаноид бериллидтерін синтездеу бойынша эксперименттерді дайындау және жүргізу кезінде вакуумдық қыздыру режимдерін негіздеуде қолданылуы мүмкін.

**Түйін сөздер:** сирек жер металдары, металл гидридтері, термодесорбциялық спектроскопия (ТДС), ұнтақ материалдар, вакуумдық қыздыру, сутегі десорбциясы.

Е. Кенжин[1], Т. Кульсартов[1], И. Кенжина[1*], Ж. Заурбекова[1],
К. Самарханов[2], С. Ударцев[1,3], А. Елишенков[1], Г. Кантай[4]
[1]НАО "КазНИТУ им. К.И.Сатпаева", Алматы, Казахстан
[2]Филиал «Институт атомной энергии» РГП НЯЦ РК, Курчатов, Казахстан
[3]АО "Ульбинский металлургический завод", Усть-каменогорск, Казахстан
[4]Институт физики Словацкой академии наук, Братислава, Словакия
*e-mail: kenzhina@physics.kz

## Термодесорбционное поведение порошков гидридов гольмия и эрбия при нагреве в вакууме

В работе исследовано термодесорбционное (ТДС) поведение порошков гидридов гольмия и эрбия при нагреве в вакууме с целью выбора обоснованных температурно-временных параметров для последующего синтеза бериллидов лантаноидов. Актуальность исследования определяется необходимостью учета газовыделения из гидридсодержащих порошковых смесей при вакуумно-термической обработке, поскольку десорбция водорода может оказывать существенное влияние на уплотнение смеси, стабильность вакуумного режима и условия фазообразования.

Перед проведением ТДС исследований выполнена характеристика исходных порошков бериллия, гидридов гольмия и эрбия, включающая анализ гранулометрического состава, морфологии частиц и фазового состояния. ТДС исследования проводились в условиях вакуума при линейном нагреве от комнатной температуры до 1173 K со скоростью 10 K/min. Показано, что при нагреве порошков гидридов гольмия и эрбия реализуется многостадийный характер с доминирующим высокотемпературным максимумом.

Полученные результаты позволяют определить температурные интервалы интенсивного газовыделения и могут быть использованы для обоснования режимов вакуумного нагрева при подготовке и проведении экспериментов по синтезу бериллидов лантаноидов из порошковых смесей на основе бериллия и редкоземельных металлов.

**Ключевые слова:** редкоземельные металлы, гидриды металлов, термодесорбционная спектроскопия (ТДС), порошковые материалы, вакуумный нагрев, десорбция водорода.

### 1. Introduction

Rare-earth metals actively interact with hydrogen to form stable hydride phases [1], which determines their important role in materials science and hydrogen energy technologies [2]. Rare-earth metal hydrides are considered promising materials for hydrogen storage [3–5], metal hydride battery anodes [6], gas sensors [7], and other functional applications [8]. For many rare-earth metals, hydrogenation is characterized by the sequential formation of two main hydride phases: the dihydride $REH_2$ and the trihydride $REH_3$, where RE represents a rare-earth metal. For elements of the yttrium subgroup, the transition from the dihydride to the trihydride is accompanied by a structural rearrangement of the crystal lattice [9–11].

The thermal stability and dehydrogenation

behavior of rare-earth metal hydrides are of practical interest, since hydrogen release during heating directly affects phase transformations [11], the state of the powder material, and the conditions under which high-temperature processes occur. According to the literature [12,13], thermal desorption of hydrogen from rare-earth metal hydrides usually proceeds in a stepwise manner and includes at least two main stages corresponding to the sequential transformations $REH_3 \rightarrow REH_2$ and $REH_2 \rightarrow RE$ [10]. For several systems, this is manifested as two distinct maxima in the thermal desorption curves during vacuum heating. This behavior has been demonstrated both in early studies on rare-earth metal hydrides [14,15] and in more recent investigations of heavy rare-earth metal hydrides [10,16].

Thus, for hydrides of heavy rare-earth metals, such as holmium and erbium, it has been shown that, during linear heating under vacuum, hydrogen desorption proceeds in two main stages: the low-temperature region is associated with the decomposition of the trihydride phase to the dihydride, whereas the high-temperature region corresponds to the further decomposition of the dihydride to the metallic state [10,16]. The positions of the desorption maxima depend on the nature of the rare-earth element and the heating conditions [10]. At the same time, most studies have focused either on general aspects of the thermodynamics and kinetics of RE–H systems [17–20] or on the investigation of hydrides as individual materials [21,22], whereas their behavior in the context of preparing starting powders for the subsequent synthesis of intermetallic compounds has been studied less.

In powder metallurgy technologies, this is of fundamental importance. When rare-earth metal hydrides are used as starting components for the synthesis of lanthanide intermetallic compounds [23,24], vacuum heating is accompanied not only by heating and densification of the mixture, but also by hydrogen release from the hydride component. This process can have a noticeable effect on the packing density of the powder mixture, the nature of contact between powder particles, the stability of vacuum conditions, and the conditions of phase formation. Therefore, before carrying out experiments on the synthesis of lanthanide beryllides, it is necessary to determine the temperature ranges of the most intense gas evolution and to assess the specific features of the thermal desorption behavior of the starting hydride powders.

The use of rare-earth metal hydrides as starting components is motivated by the strong oxygen affinity of rare-earth metals and their tendency to oxidize rapidly in the metallic state, which makes handling pure metal powders difficult. In this regard, the hydride form is considered a more oxidation-resistant alternative. At the same time, the presence of hydrogen and its release during heating can affect subsequent processes, including phase formation and the selection of temperature–time parameters for heat treatment. Therefore, in the present work, in addition to thermal desorption studies, a preliminary characterization of the starting holmium and erbium hydride powders was performed, including analysis of particle size distribution, particle morphology, and phase state.

The aim of this work is to establish the specific features of the thermal desorption behavior of holmium and erbium hydride powders during vacuum heating in order to select justified temperature–time parameters for the subsequent synthesis of lanthanide beryllides.

## Materials and Methods

*Starting Materials*

Holmium and erbium hydride powders with a declared purity of 99.5% were used as the starting rare-earth components. The total content of metallic impurities, including Tb, Dy, Tm, Y, Ca, Si, Fe, Al, and C, did not exceed 0.2 wt.%. The holmium and erbium hydride powders were used as received, without additional purification or pretreatment.

The results of the particle size distribution, particle morphology, and phase composition analyses of the starting powders are presented and discussed in Section 3.1.

*Characterization methods*

Particle size analysis was performed using an Analysette 22 NanoTec (Fritsch GmbH) laser particle sizer.

The phase composition of the starting powders was studied by X-ray diffraction (XRD) using a Bruker D8 Advance Eco diffractometer. Phase identification was performed using the ICDD PDF-2 database. The list of reference diffraction cards used for phase identification is given in Table 1.

Microstructural characterization of the starting powders was performed using a JEOL JSM-5610 scanning electron microscope (SEM). The analysis was conducted in secondary electron (SE) mode to examine the surface topography and in backscattered electron (BSE) mode to obtain compositional contrast.

**Table 1.** ICDD PDF2-2021 material card numbers used for XRD analysis interpretation

| Compound name | ICDD PDF2 Card Number | Pearson Symbol, Space Group | Lattice Parameters |
|---|---|---|---|
| Ho | 01-071-4991 | Hexagonal, hP2, P63/mmc (194) | a = b=3.576, c = 5.614 α=β=90°, γ=120° $V_{cr.lat.}$ = 62.18 |
| $HoH_2$ | 03-065-7209 | Cubic cI12, Fm-3m (225) | a = b = c = 5.165, α=β=γ=90° $V_{cr.lat.}$ = 137.79 |
| Er | 03-065-7248 | Hexagonal, hP2, P63/mmc (194) | a = b=3.593, c = 5.681 α=β=90°, γ=120° $V_{cr.lat.}$ = 63.51 |
| $ErH_2$ | 00-060-0141 | Cubic cI12, Fm-3m (225) | a = b = c = 5.129, α=β=γ=90° $V_{кр.реш.}$ = 134.91 |
| $Er_2O_3$ | 00-008-0050 | Cubic cI12, Ia-3 (206) | a = b = c = 10.548, α=β=γ=90° $V_{кр.реш.}$ = 117.57 |

*TDS experiments*

To investigate the thermal desorption behavior of holmium and erbium hydride powders during vacuum heating, an experimental setup with an experimental device was used; a detailed description of this setup is given in [25,26].

Samples of holmium and erbium hydride powders weighing 231.85 mg and 165.82 mg, respectively, were loaded into an $Al_2O_3$ ceramic crucible equipped with a port for a type-K thermocouple, which enabled sample temperature monitoring during the experiment.

Gas evolution from the rare-earth metal hydride powders was monitored in real-time using an RGA-100 quadrupole mass spectrometer (SRS).

Thermal desorption spectra were recorded during linear heating of the samples from room temperature to 1173 K at a heating rate of 10 K/min. The experiments were carried out under high-vacuum conditions; the initial pressure before the measurements was $1 \cdot 10^{-6}$ Torr and was maintained using a turbomolecular pump.

## Results and discussion

*Particle size distribution of the starting powders*

The particle size distribution of the holmium hydride powder is shown in Figure 1.

The particle size ranges from 14 to 70 μm. The distribution is continuous and does not exhibit any narrowly defined maxima. The average particle size of the holmium hydride powder is 42.36 μm.

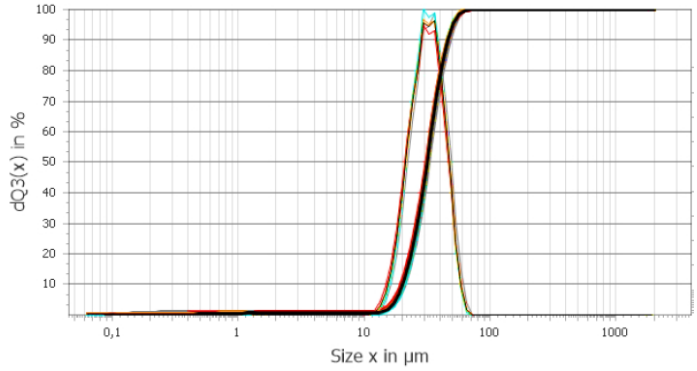


**Figure 1 –** Particle size distribution of holmium hydride powder

The particle size distribution of the erbium hydride powder is shown in Figure 2. In contrast to the holmium hydride powder, the erbium hydride powder is characterized by a broader and more heterogeneous distribution and is significantly finer. The particle size varies over a wide range from 0.1 to 28 μm. Three size regions can be distinguished in the particle size distribution curve: below 1 μm, 1–5 μm, and 5–28 μm. Overall, the average particle size of the erbium hydride powder is 7.22 μm.

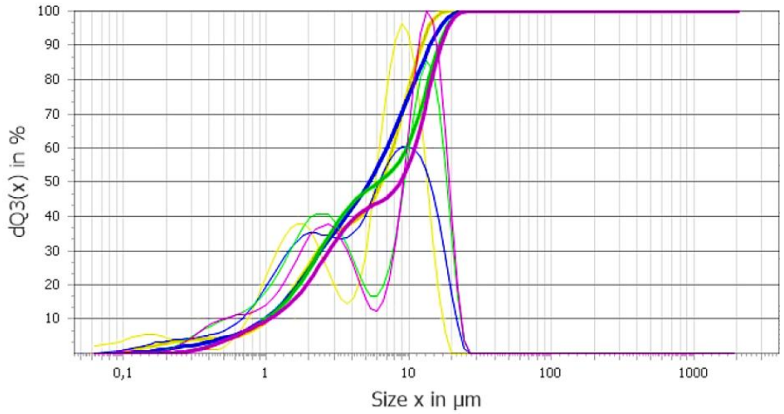


**Figure 2 –** Particle size distribution of erbium hydride powder

*Morphology of the starting powders*

The particle morphology of the starting holmium and erbium hydride powders is shown in Figures 3 and 4.

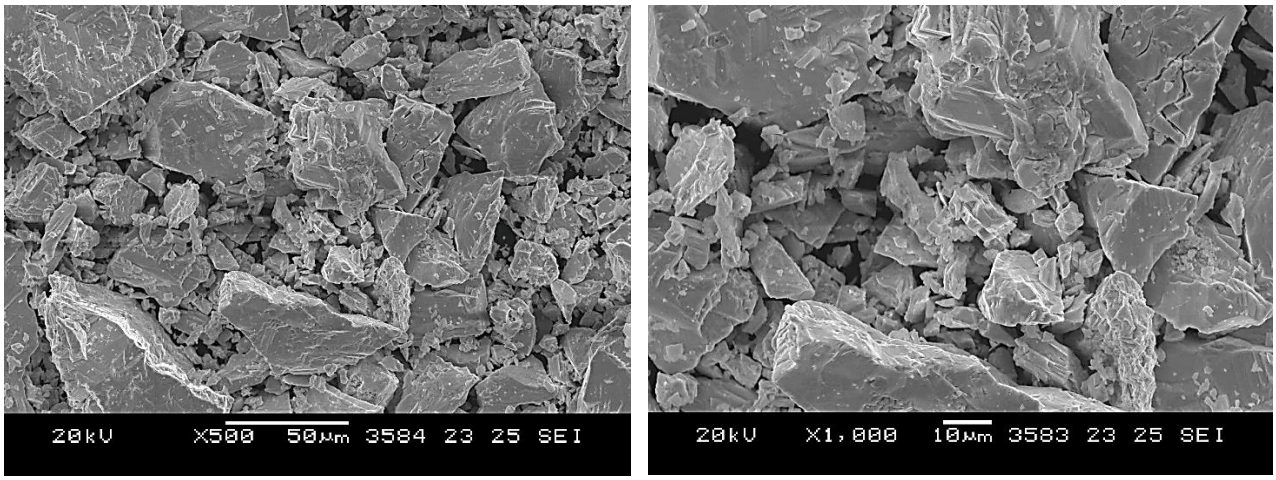


**Figure 3 –** SEM images of the starting holmium hydride powder at different magnifications

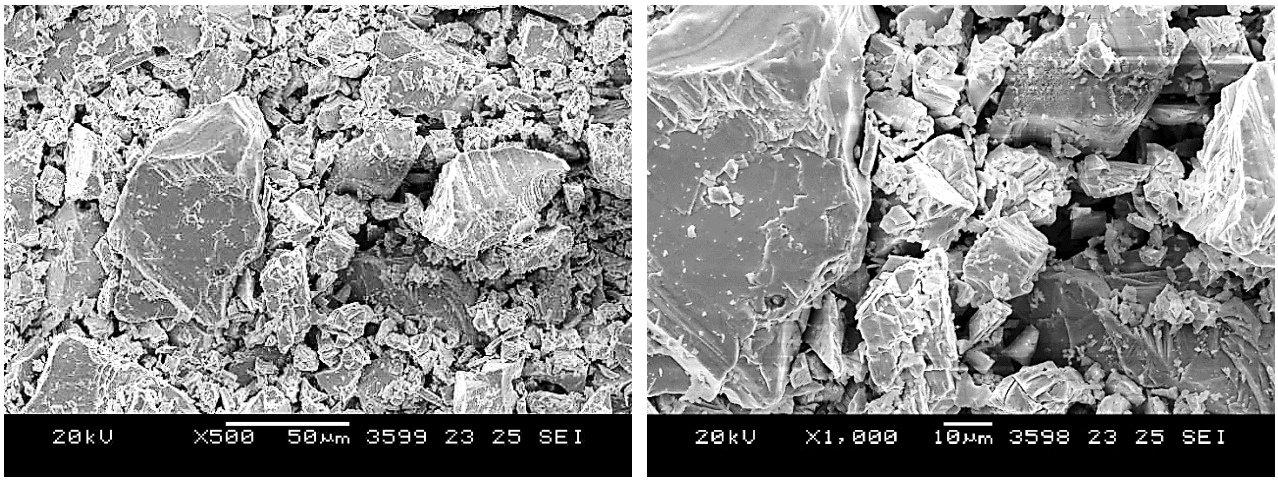


**Figure 4 –** SEM images of the starting erbium hydride powder at different magnifications

Both powders consist predominantly of irregularly shaped particles with angular outlines, sharp edges, and flat fracture surfaces. Such morphology is typical of brittle hydride materials. No pronounced internal porosity is observed in the investigated particles. At the same time, the SEM images clearly reveal a difference in particle size: the holmium hydride powder is represented by larger particles, whereas the erbium hydride powder contains finer fragments, which is consistent with the results of the particle size analysis.

*Phase composition of the starting powders*

The results of the XRD analysis of the starting holmium and erbium hydride powders are shown in Figures 5 and 6.

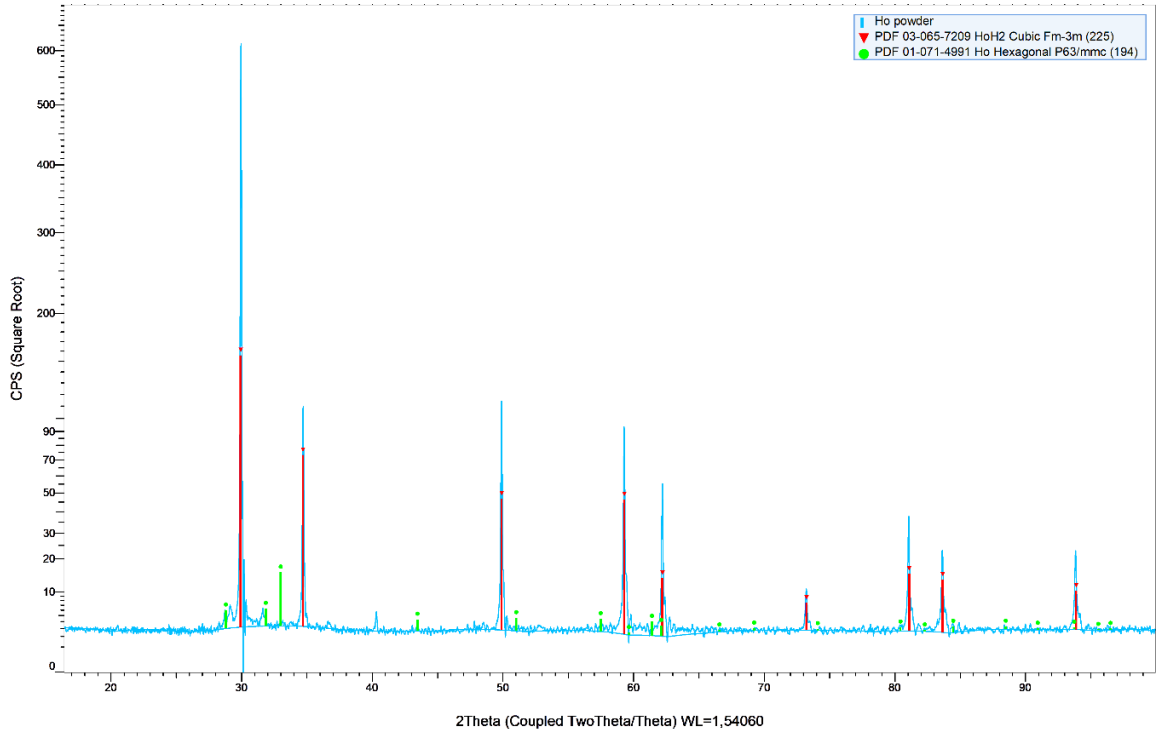


**Figure 5**– XRD patterns for the starting holmium hydride powder

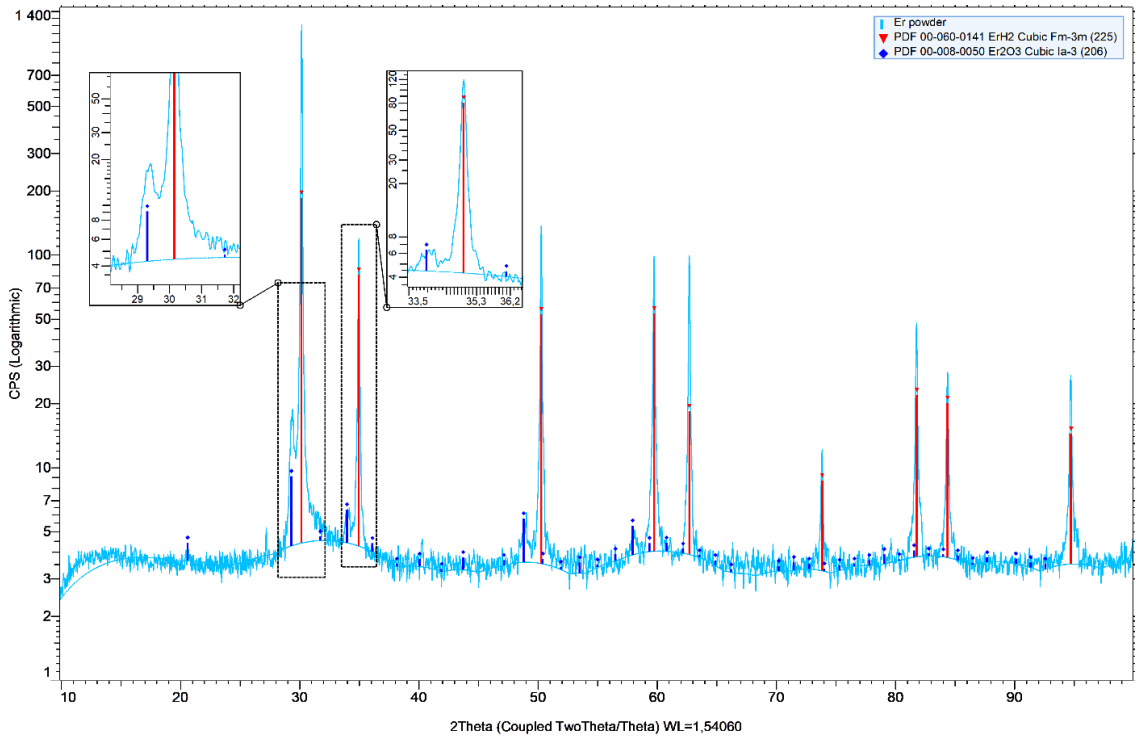


**Figure 6 –** XRD patterns for the starting erbium hydride powder

The XRD pattern of the holmium hydride powder (see Figure 5) is characterized by the predominance of reflections corresponding to the cubic $HoH_2$ phase. Reflections of metallic holmium are either absent or have extremely low intensity, indicating that the rare-earth component is predominantly present in the hydride form.

The XRD pattern of the erbium hydride powder (see Figure 6) is characterized by the presence of two phases: erbium hydride $ErH_2$ with a cubic Fm-3m structure and erbium oxide $Er_2O_3$ with a cubic Ia-3 structure.

*Thermal desorption behavior of holmium and erbium hydride powders upon vacuum heating*

The overall evolution of the sample temperature and the partial pressures of gaseous components during the TDS experiments with holmium and erbium hydride powders, as well as for the empty alumina crucible, is shown in Figure 7. It can be seen that gas evolution from both investigated powders is qualitatively similar, has a multistage character, and differs markedly from the background signal of the empty crucible.

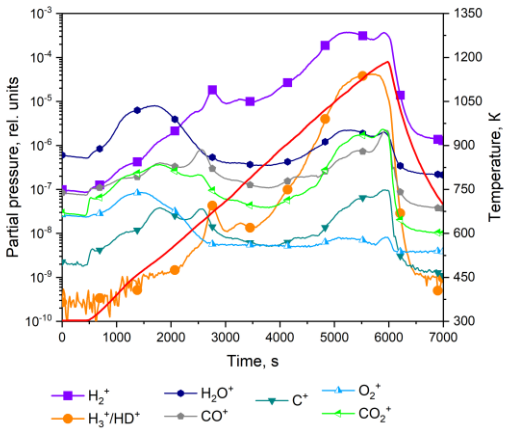


a) gas evolution from the holmium hydride powder

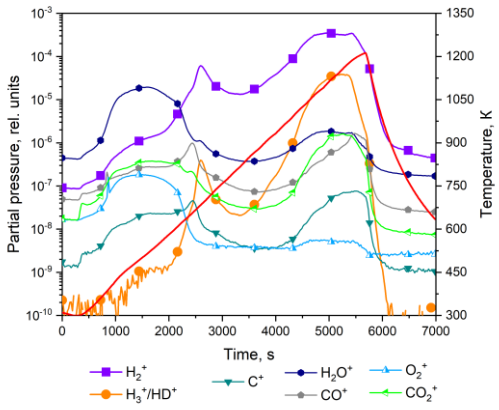


b) gas evolution from the erbium hydride powder

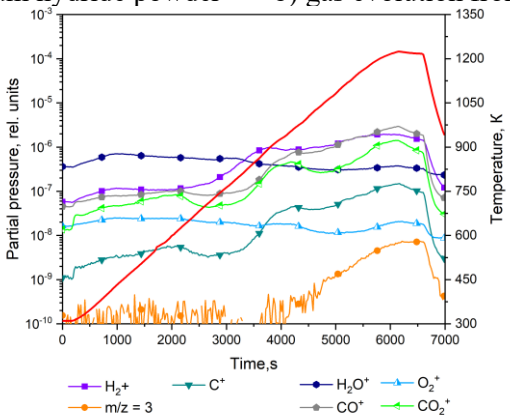


c) empty crucible

**Figure 7**– Time dependences of the partial pressures of gaseous species in the volume of the experimental device during the TDS experiment

Figure 8 presents a diagram of the contributions of gaseous products during linear heating of the investigated holmium and erbium hydride samples, allowing a clearer comparison of the role of individual components in the total gas evolution from the samples. In both cases, hydrogen-containing components account for a major part of the gas release. For the holmium hydride powder, the contribution of molecular hydrogen is 89.63%, while that of the accompanying signal at $m/z = 3$ is 6.66%, together accounting for 96.29% of the total gas evolution. For the erbium hydride powder, the corresponding values are 86.63% and 5.75%, respectively, and the total contribution of these two components is 92.38%. Among the impurity components, water vapor is the most significant, amounting to 2.38% for the holmium hydride powder and 6.07% for the erbium hydride powder, respectively. The contributions of CO and $CO_2$ are 0.75% and 0.61%, respectively; $O_2$, 0.17% and 0.24%; carbon-containing components, 0.04% for both powders; and other products, 0.37% and 0.67%, respectively. Thus, hydrogen determines the overall pattern of thermal desorption for both investigated

powders, whereas the other gases make only minor contributions.

It should be noted that the nature of the signal at $m/z = 3$, whose temperature dependence qualitatively follows the main stages of $m/z = 2$ (molecular hydrogen $H_2^+$) release, cannot be clearly established based solely on the RGA-100 mass spectrometer data. Its appearance is likely associated with the overlap of several contributions. On the one hand, under conditions of intense $H_2^+$ evolution and an increase in pressure in the volume of the experimental device to approximately $10^{-4}$–$2 \cdot 10^{-4}$ Torr, $H_3^+$ ions may be formed and detected in the ion source of the mass spectrometer as a result of ion–molecule processes involving $H_2$. On the other hand, contribution from $HD^+$ ions cannot be excluded, since TDS experiments with deuterium-purged samples had previously been performed in the same vacuum chamber [25,26]. In this case, the $m/z = 3$ signal may be attributed to residual deuterium retained in the vacuum system, its desorption from chamber components, and subsequent isotopic exchange with hydrogen released from the investigated hydrides. Additional contributions may also arise from hydrogen-containing impurity fragments associated with the production and storage conditions of the powders. Therefore, in the present work, the $m/z = 3$ signal is not considered an independent indicator of a separate phase or dehydrogenation stage, but rather as an accompanying hydrogen-containing signal reflecting the combined contribution of $H_3^+$, $HD^+$, and possible impurity components. The observed change in the ratio of the $m/z = 2$ and $m/z = 3$ signals in the high-temperature region above 900 K is apparently related to the combined effect of the increasing $H_2$ from the hydride phase and the activation of high-temperature desorption/isotopic exchange of residual deuterium in the components of the vacuum system.

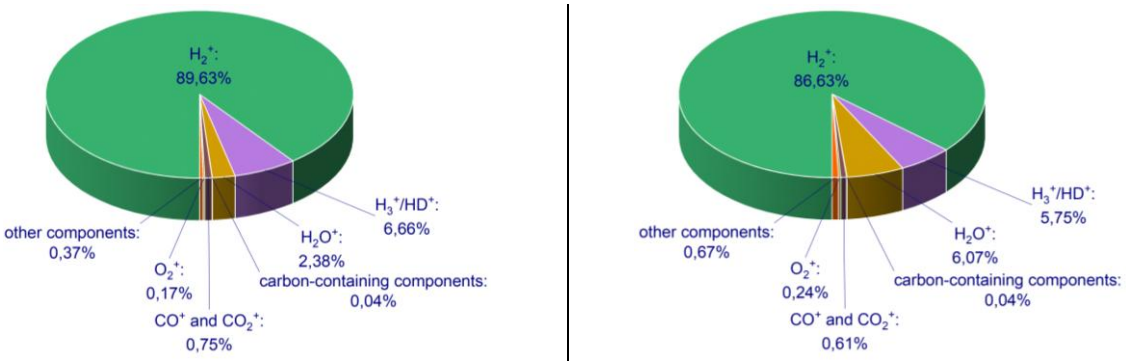


a) Ho sample b) Er sample

**Figure 8**– Contribution of gaseous components to the total gas evolution during linear heating of the investigated samples

It should be noted that, despite the overall dominance of $H_2^+$, the distribution of impurity components differs somewhat between the holmium and erbium hydride powders. In particular, the erbium hydride powder exhibits a higher contribution of water vapor compared with the holmium hydride powder. This may be related to the previously established difference in the dispersity of the starting powders: erbium hydride is a significantly finer material and therefore has a more developed surface capable of retaining a larger amount of adsorbed species.

The temperature dependences of the total pressure in the volume of the experimental device containing the investigated sample during linear heating under vacuum at a rate of 10 K/min are shown in Figure 9.

The main parameters for the gas release of hydrogen-containing components are summarized in Table 2.

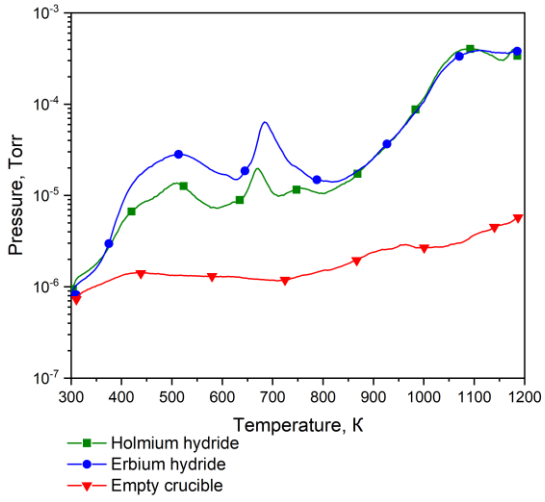


**Figure 9** – Temperature dependences of the total pressure in the volume of the ampoule device containing the investigated sample during linear heating under vacuum at a rate of 10 K/min.

.

**Table 2.** Parameters of hydrogen-containing component release

| Sample | Sample mass, mg | Component | Peak | Temperature range and peak maximum, K | | Amount of released gas, mol | Number of released atoms |
|---|---|---|---|---|---|---|---|
| Ho | 231.85 | *m/z* = 2 | 1 Peak | onset | 625 | 6.14E-06 | 3.70E+18 |
| | | | | peak | 670 | | |
| | | | | end | 710 | | |
| | | | 2 Peak | onset | 710 | 4.92E-06 | 2.96E+18 |
| | | | | peak | 755 | | |
| | | | | end | 795 | | |
| | | | 3 Peak | onset | 795 | 3.41E-04 | 2.05E+20 |
| | | | | peak | 1085 | | |
| | | | | end | 1158 | | |
| | | *m/z* = 3 | 1 Peak | onset | 625 | 1.03E-08 | 6.19E+15 |
| | | | | peak | 670 | | |
| | | | | end | 710 | | |
| | | | 2 Peak | onset | 710 | 6.95E-09 | 4.19E+15 |
| | | | | peak | 755 | | |
| | | | | end | 795 | | |
| | | | 3 Peak | onset | 795 | 2.43E-05 | 1.46E+19 |
| | | | | peak | 1085 | | |
| | | | | end | 1158 | | |
| Er | 165.82 | *m/z* = 2 | 1 Peak | onset | 560 | 2.77E-05 | 1.67E+19 |
| | | | | peak | 685 | | |
| | | | | end | 820 | | |
| | | | 2 Peak | onset | | - | - |
| | | | | peak | no | | |
| | | | | end | | | |
| | | | 3 Peak | onset | 815 | 3.06E-04 | 1.84E+20 |
| | | | | peak | 1110 | | |
| | | | | end | 1165 | | |
| | | *m/z* = 3 | 1 Peak | onset | 590 | 9.57E-08 | 5.76E+16 |
| | | | | peak | 685 | | |
| | | | | end | 820 | | |
| | | | 2 Peak | onset | | - | - |
| | | | | peak | no | | |
| | | | | end | | | |
| | | | 3 Peak | onset | 815 | 2.05E-05 | 1.24E+19 |
| | | | | peak | 1110 | | |
| | | | | end | 1165 | | |

Analysis of the temperature dependences of the partial pressures shows that gas evolution from the $HoH_x$ and $ErH_x$ powders has a multistage character. In the initial heating region, approximately 380–600 K, the main contribution to the gas phase is made by water vapor and oxygen-containing components. This region is most likely associated with the removal of physically adsorbed moisture, degassing of the particle surfaces, and the release of weakly bound surface compounds.

In the medium-temperature region of 650–820 K, the contribution of hydrogen-containing components increases. For the $HoH_x$ powder, two partially separated maxima are observed in this region at 670 and 755 K, whereas for the $ErH_x$ powder, one broader maximum is recorded at 685 K. This difference may be related to differences in the initial phase state, powder dispersity, and the degree of overlap between individual dehydrogenation stages.

The most intense hydrogen release for both powders is observed in the high-temperature region above 800 K. The main maxima of the *m/z* = 2 signal are located at 1085 K for $HoH_x$ and 1110 K for $ErH_x$. This stage accounts for the major part of $H_2^+$ gas

evolution and correlates well with the increase in the total pressure in the chamber volume shown in Figure 9. This maximum can be associated with the decomposition of the most stable hydride component, which is consistent with literature data on the thermal desorption of heavy rare-earth metal hydrides. For the interpretation of the observed multistage behavior, it is essential to consider the difference between the present work and study [10]. In [10], the objects of investigation were rare-earth metal dihydrides and trihydrides preliminarily hydrogenated under controlled conditions, and TDS measurements were conducted for these materials at several heating rates. In the present work, the starting holmium and erbium hydride powders were investigated as received, without additional purification or pretreatment.

The obtained results should be discussed considering the phase behavior of the Ho-H [18] and Er-H [19] systems. According to the literature data, both systems are characterized by the existence of several hydride states depending on hydrogen content and temperature. For the Ho-H system, the possible existence of a solid-solution region, as well as states close to the dihydride and trihydride regions, has been established [18]. For the Er-H system, complex phase behavior and the presence of several homogeneity regions depending on hydrogen content and thermodynamic conditions have also been reported [19]. $H_2^+$ is released into the gas phase, whereas sequential transformations from more hydrogen-rich to less hydrogen-rich states occur in the solid phase. From this viewpoint, the medium-temperature region can be qualitatively associated with the transition from more hydrogen-rich hydride states to less hydrogen-rich ones, while the high-temperature maximum can be attributed to the decomposition of the most stable hydride component. This interpretation is also consistent with the XRD results for the starting powders, in which the $HoH_2$ and $ErH_2$ hydride phases dominate, with minor oxide phases present.

The obtained results are generally consistent with literature data on the thermal desorption of heavy rare-earth metal hydrides. In [10], two main hydrogen desorption stages were identified for Ho and Er hydrides: a low-temperature stage associated with the transition from a more hydrogen-rich state to a less hydrogen-rich one, and a high-temperature stage corresponding to the further decomposition of the hydride phase. The high-temperature peaks for Ho- and Er-containing systems were reported to occur in the range of 1083–1159 K. The temperatures of the main high-temperature maxima obtained in the present work, approximately 1085 K for holmium hydride and approximately 1110 K for erbium hydride, are in good agreement with this temperature range. At the same time, the low- and medium-temperature parts of the desorption curves in the present work have a more complex shape than those reported in [10], which is apparently related to differences in the initial state of the investigated materials: particularly, prepared rare-earth metal dihydride and trihydride powders were studied in [10], whereas the present work deals with starting hydride powders.

A comparison with [16], in which thermal desorption of erbium hydride was considered taking into account phase-structural transformations, is also of interest. That study showed that decomposition of the hydride phase is accompanied by sequential dehydrogenation stages and may be established in a complex shape of the desorption curves. In the present work, the $m/z = 3$ signal is not considered an independent basis for interpreting phase transformations; however, its presence provides additional support for the multistage character of hydrogen gas evolution.

## Conclusion

The thermal desorption behavior of the starting holmium and erbium hydride powders during linear heating under vacuum was investigated. It was established that gas release from both powders has a multistage character, with hydrogen-containing components making the main contribution to the total gas evolution. The most intense hydrogen release from the holmium and erbium hydride powders occurs in the high-temperature region, with maxima at 1085 K and 1110 K, respectively, whereas the low- and medium-temperature stages are associated with the removal of surface-bound impurities and the onset of dehydrogenation of more hydrogen-rich states. The observed differences in gas evolution behavior between the investigated powders are consistent with differences in their dispersity and initial phase state.

The obtained results provide an experimental basis for the further selection of vacuum heating regimes for the synthesis of lanthanide beryllides and make it possible to take into account the influence of the hydride component on the gas dynamics of the process, phase formation conditions, and billets preparation.

**Acknowledgments**

The research was funded by the Science Committee of the Ministry of Science and Higher Education of the Republic of Kazakhstan with Grant No. AP26104425.

**Author Contributions**

**Ye. Kenzhin**: Conceptualization, Methodology, Investigation; **T. Kulsartov**: Writing – Original Draft; **I.Kenzhina**: Writing – Original Draft, Supervision, Funding Acquisition, Project Administration; **Zh. Zaurbekova**: Writing – Review & Editing; **K. Samarkhanov**: Writing – Original Draft, Investigation; **S. Udartsev**: Investigation; **A. Yelishenkov**: Investigation; **G. Kantay**: Investigation.

## References


1. V.A. Yartys, E. Akiba, R.C. Bowman, Jr., C.E. Buckley, J. Graetz, M. Hirscher, M. Paskevicius, M. Zhu, T. Gennett, T. Autrey, and V. Stavila, Metal hydrides: a historical perspective, *J. Alloys Compd.* **1050**, 185734 (2026). https://doi.org/10.1016/j.jallcom.2025.185734
2. Y. Xu, X. Yang, Y. Li, Y. Zhao, X. Shu, G. Zhang, T. Yang, Y. Liu, P. Wu, and Z. Ding, Rare-earth metal-based materials for hydrogen storage: progress, challenges, and future perspectives, *Nanomaterials* **14**, 1671 (2024). https://doi.org/10.3390/nano14201671
3. X. Wang, F. Zhu, X. Xue, T. He, Y. Zhang, G. Tao, Y. Zhang, H. Wang, and Y. Liu, Suction-cast strategy to enhance hydrogen storage performance of rare earth-based alloys, *Int. J. Hydrogen Energy* **104**, 220–227 (2025). https://doi.org/10.1016/j.ijhydene.2024.04.327
4. V.A. Yartys, Metal Hydrides for Hydrogen-Based Energy Storage, Volume 1: Fundamentals, Vol. 1 (Elsevier, 2025), pp. 1–391. https://doi.org/10.1016/C2023-0-52445-0
5. V.A. Yartys, Metal Hydrides for Hydrogen-Based Energy Storage, Volume 2: Applications, Vol. 2 (Elsevier, 2025), pp. 1–513. https://doi.org/10.1016/C2025-0-01811-2
6. R. Griessen, J. N. Huiberts, M. Kremers, A. T. M. van Gogh, N. J. Koeman, J. P. Dekker, and P. H. L. Notten, Yttrium and lanthanum hydride films with switchable optical properties, *J. Alloys Compd.* **253–254**, 44–50 (1997). https://doi.org/10.1016/S0925-8388(96)02891-5
7. M.V. Lototskyy, B.P. Tarasov, and V.A. Yartys, Gas-phase applications of metal hydrides, *J. Energy Storage* **72**, 108165 (2023). https://doi.org/10.1016/j.est.2023.108165
8. V.A. Yartys, M.V. Lototskyy, V. Linkov, S. Pasupathi, M.W. Davids, I. Tolj, G. Radica, R.V. Denys, J. Eriksen, K. Taube, J. Bellosta von Colbe, G. Capurso, M. Dornheim, F. Smith, D. Mathebula, D. Swanepoel, and S. Suwarno, HYDRIDE4MOBILITY: an EU HORIZON 2020 project on hydrogen-powered fuel cell utility vehicles using metal hydrides in hydrogen storage and refuelling systems, *Int. J. Hydrogen Energy* **46**, 35896–35909 (2021). https://doi.org/10.1016/j.ijhydene.2021.01.190
9. L.C. Beavis, Characteristics of some binary transition metal hydrides, *J. Less-Common Met.* **19**, 315–328 (1969). https://doi.org/10.1016/0022-5088(69)90177-5
10. S. Suwarno, M.V. Lototskyy, and V.A. Yartys, Thermal desorption spectroscopy studies of hydrogen desorption from rare earth metal trihydrides REH3 (RE = Dy, Ho, Er), *J. Alloys Compd.* **842**, 155530 (2020). https://doi.org/10.1016/j.jallcom.2020.155530
11. H. Meng, M.A. Kuzovnikov, and M. Tkacz, Phase stability of some rare earth trihydrides under high pressure, *Int. J. Hydrogen Energy* **42**, 29344–29349 (2017). https://doi.org/10.1016/j.ijhydene.2017.10.067
12. R.C. Bowman, Jr., Metal deuterides and tritides, in *Metal Hydrides for Hydrogen-Based Energy Storage*, Vol. 1, pp. 171–204 (Woodhead Publishing, 2026). https://doi.org/10.1016/B978-0-443-33370-5.00015-5
13. F.J. Castro and G. Meyer, Thermal desorption spectroscopy (TDS) method for hydrogen desorption characterization (I): theoretical aspects, *J. Alloys Compd.* **330–332**, 59–63 (2002). https://doi.org/10.1016/S0925-8388(01)01625-5
14. P. S. Rudman, Hydrogen-diffusion-rate-limited hydriding and dehydriding kinetics, *J. Appl. Phys.* **50**, 7195–7199 (1979). https://doi.org/10.1063/1.325831
15. V.A. Yartys, O. Gutfleisch, V.V. Panasyuk, and I.R. Harris, Desorption characteristics of rare earth (R) hydrides (R = Y, Ce, Pr, Nd, Sm, Gd, and Tb) in relation to the HDDR behaviour of R–Fe-based compounds, *J. Alloys Compd.* **253–254**, 128–133 (1997). https://doi.org/10.1016/S0925-8388(96)03097-6
16. M. Ma, L. Wang, R. Wan, B. Tang, and X. Tan, Phase-structural transformation of erbium trihydride studied by thermal desorption spectroscopy, *Int. J. Hydrogen Energy* **48**, 13913–13921 (2023). https://doi.org/10.1016/j.ijhydene.2022.12.328
17. W.L. Korst and J.C. Warf, Rare earth-hydrogen systems. I. Structural and thermodynamic properties, *Inorg. Chem.* **5**, 1719–1726 (1966). https://doi.org/10.1021/ic50044a018
18. F.C. Perkins and C.E. Lundin, The holmium-hydrogen system, *J. Electrochem. Soc.* **115**, 21 (1968). https://doi.org/10.1149/1.2410992
19. A. Mascaro, C. Toffolon-Masclet, C. Raepsaet, and J.-M. Joubert, Experimental study and thermodynamic assessment of the erbium–hydrogen binary system, *Calphad* **41**, 50–59 (2013). https://doi.org/10.1016/j.calphad.2013.01.004
20. J. Šesták and G. Berggren, Study of the kinetics of the mechanism of solid-state reactions at increasing temperatures, *Thermochim. Acta* **3**, 1–12 (1971). https://doi.org/10.1016/0040-6031(71)85051-7

21. I. Gabis, E. Evard, A. Voyt, I. Chernov, and Y. Zaika, Kinetics of decomposition of erbium hydride, *J. Alloys Compd.* **356–357**, 353–357 (2003). https://doi.org/10.1016/S0925-8388(02)01230-6

22. I.E. Gabis, A.P. Voit, E.A. Evard, Y.V. Zaika, I.A. Chernov, and V. . Yartys, Kinetics of hydrogen desorption from the powders of metal hydrides, *J. Alloys Compd.* **404–406**, 312–316 (2005). https://doi.org/10.1016/j.jallcom.2005.02.090

23. A. Amon, Rare earth and actinide beryllides: structural chemistry and physical properties, in *Handbook on the Physics and Chemistry of Rare Earths*, Vol. 59, edited by R. J. M. Konings (Elsevier, 2021), pp. 93–140. https://doi.org/10.1016/bs.hpcre.2021.04.001

24. E. Bucher, D.J. Lockwood, and K.H.J. Buschow, Electronic properties of beryllides of the rare earth and some actinides, *Phys. Rev. B* **11**, 440–451 (1975). https://doi.org/10.1103/PhysRevB.11.440

25. Y. Kenzhin, I. Kenzhina, T. Kulsartov, Z. Zaurbekova, S. Askerbekov, Y. Ponkratov, Y. Gordienko, A. Yelishenkov, S. Udartsev, Study of hydrogen sorption and desorption processes of zirconium beryllide $ZrBe_2$, *Nuclear Materials and Energy,* **39**, 101634 (2024). https://doi.org/10.1016/j.nme.2024.101634

26. I E. Kenzhina, T.V. Kulsartov, Ye.V. Chikhray, Zh.A. Zaurbekova, Yu.V. Ponkratov, A.L. Kozlovskiy, A.B. Yelishenkov, S.K. Askerbekov, and A.U. Tolenova, Investigation of tin-lithium alloy behavior in high-temperature hydrogen isotope environments: sorption and desorption analysis, *Bull. L.N. Gumilyov Eurasian Natl. Univ., Phys. Astron. Ser.* **150**, 162–185 (2025). https://doi.org/10.32523/2616-6836-2025-150-1-162-185

***Information about authors:***

*Yergazy Kenzhin – Candidate of physical and mathematical sciences, Leading researcher, Satbayev University, (Almaty, Kazakhstan, e-mail: keakmay@gmail.com).*

*Timur Kulsartov – Candidate of physical and mathematical sciences, PhD, Leading researcher, Satbayev University, (Almaty, Kazakhstan, e-mail: tima@physics.kz).*

*Inesh Kenzhina (corresponding author) – PhD, Leading researcher, Satbayev University, (Almaty, Kazakhstan, e-mail: kenzhina@physics.kz).*

*Zhanna Zaurbekova – PhD Candidate, Senior researcher, Satbayev University, (Almaty, Kazakhstan, e-mail: zzha@physics.kz).*

*Kuanysh Samarkhanov – Senior researcher, Institute of Atomic Energy Branch of the National Nuclear Center of the Republic of Kazakhstan, (Kurchatov, Kazakhstan, e-mail: samarkhanov@nnc.kz).*

*Sergey Udartsev – Postgraduate, Leading researcher, Satbayev University, (Almaty, Kazakhstan, e-mail: udartsevsv@ulba.kz).*

*Alexandr Yelishenkov – researcher, Satbayev University, (Almaty, Kazakhstan, e-mail: aleksandrelisenkov282@gmail.com).*

*Gulnur Kantay – Senior researcher, Institute of Physics of the Slovak Academy of Sciences, (Bratislava, Slovakia, e-mail: 22kantai@gmail.com). https://orcid.org/0000-0001-8366-8521*

***Авторлар туралы мәлімет:***

*Ерғазы Кенжин – физика-математика ғылымдарының кандидаты, жетекші ғылыми қызметкер, Қ.И. Сәтбаев атындағы ҚазҰТЗУ КеАҚ, (Алматы, Қазақстан, e-mail: keakmay@gmail.com).*

*Тимур Кульсартов – физика-математика ғылымдарының кандидаты, PhD, жетекші ғылыми қызметкер, Қ.И. Сәтбаев атындағы ҚазҰТЗУ КеАҚ, (Алматы, Қазақстан, e-mail: tima@physics.kz).*

*Инеш Кенжина (автор-корреспондент) – PhD, жетекші ғылыми қызметкер, Қ.И. Сәтбаев атындағы ҚазҰТЗУ КеАҚ, (Алматы, Қазақстан, e-mail: kenzhina@physics.kz).*

*Жанна Заурбекова – докторант, аға ғылыми қызметкер, Қ.И. Сәтбаев атындағы ҚазҰТЗУ КеАҚ, (Алматы, Қазақстан, e-mail: zzha@physics.kz).*

*Қуаныш Самарханов – аға ғылыми қызметкер, Қазақстан Республикасы Ұлттық ядролық орталығының Атом энергиясы институты филиалы, (Курчатов, Қазақстан, e-mail: samarkhanov@nnc.kz).*

*Сергей Ударцев – аспирант, жетекші ғылыми қызметкер, Қ.И. Сәтбаев атындағы ҚазҰТЗУ КеАҚ, (Алматы, Қазақстан, e-mail: udartsevsv@ulba.kz).*

*Александр Елишенков – ғылыми қызметкер, Қ.И. Сәтбаев атындағы ҚазҰТЗУ КеАҚ, (Алматы, Қазақстан, e-mail: aleksandrelisenkov282@gmail.com).*

*Гүлнұр Қантай – аға ғылыми қызметкер, Словакия ғылым академиясының Физика институты, (Братислава, Словакия, e-mail: 22kantai@gmail.com).*

***Сведения об авторах:***

*Ергазы Кенжин – кандидат физико-математических наук, ведущий научный сотрудник, НАО "КазНИТУ им. К.И.Сатпаева", (Алматы, Казахстан, e-mail: keakmay@gmail.com).*

*Тимур Кульсартов – кандидат физико-математических наук, PhD, ведущий научный сотрудник, НАО "КазНИТУ им. К.И.Сатпаева", (Алматы, Казахстан, e-mail: tima@physics.kz).*

*Инеш Кенжина (автор-корреспондент) – PhD, ведущий научный сотрудник, НАО "КазНИТУ им. К.И.Сатпаева", (Алматы, Казахстан, e-mail: kenzhina@physics.kz).*

*Жанна Заурбекова – докторант, старший научный сотрудник, НАО "КазНИТУ им. К.И.Сатпаева", (Алматы, Казахстан, e-mail: zzha@physics.kz).*

*Куаныш Самарханов – старший научный сотрудник, филиал Институт атомной энергии Национального ядерного центра Республики Казахстан, (Курчатов, Казахстан, e-mail: samarkhanov@nnc.kz).*

*Сергей Ударцев – аспирант, ведущий научный сотрудник, НАО "КазНИТУ им. К.И.Сатпаева", (Алматы, Казахстан, e-mail: udartsevsv@ulba.kz).*

*Александр Елишенков – научный сотрудник, НАО "КазНИТУ им. К.И.Сатпаева", (Алматы, Казахстан, e-mail: aleksandrelisenkov282@gmail.com).*

*Гульнур Кантай – старший научный сотрудник, Институт физики Словацкой академии наук, (Братислава, Словакия, e-mail: 22kantai@gmail.com).*

***Article history:*** *received: 12 May 2026; revised: 20 July; accepted: 28 July 2026.*

***Мақала тарихы:*** *түсті: 12 мамыр 2026; түзетілді:20 шілде; қабылданды: 28 шілде 2026.*

***История статьи:*** *поступила: 12 мая 2026; после доработки: 20 июля; принята: 28 июля 2026.*